

7-12-2020

## EMHD Mixed Convection Flow through Saturated Porous Rectangular Channel.

A. Kabeel

*Mechanical power engineering dept., Faculty of engineering, Tanta University, Egypt*

M. El-kady

*Mechanical power engineering dept., Faculty of engineering, Mansoura University, Egypt*

E. El-Agouz

*Mechanical power engineering dept., Faculty of engineering, Tanta University, Egypt*

M. Amro

S. Dafea

*Mechanical power engineering dept., Faculty of engineering, Tanta University, Egypt*

Follow this and additional works at: <https://mej.researchcommons.org/home>

---

### Recommended Citation

Kabeel, A.; El-kady, M.; El-Agouz, E.; Amro, M.; and Dafea, S. (2020) "EMHD Mixed Convection Flow through Saturated Porous Rectangular Channel.," *Mansoura Engineering Journal*: Vol. 40 : Iss. 4 , Article 11. Available at: <https://doi.org/10.21608/bfemu.2020.102391>

This Original Study is brought to you for free and open access by Mansoura Engineering Journal. It has been accepted for inclusion in Mansoura Engineering Journal by an authorized editor of Mansoura Engineering Journal. For more information, please contact [mej@mans.edu.eg](mailto:mej@mans.edu.eg).

# Emhd mixed convection flow through saturated porous rectangular channel

## الحمل المختلط خلال قناة أفقية مستطيلة مشبعة بمادة مسامية تحت تأثير مجال كهرومغناطيسي

A. E.Kabeel<sup>b</sup>, M. S. El-kady<sup>a</sup>, E. A. El-Agouz<sup>b</sup> M. I. Amro<sup>b</sup> and S. Dafea<sup>b</sup>  
a- Mansoura University, Egypt, b- Mechanical power engineering dept., Faculty of engineering, Tanta University, Egypt

### الملخص

تم عمل موديل عددي لسريان الموائع الموصلة للتيار الكهربى تحت تأثير المجالات الكهرومغناطيسية باستخدام ديناميكا الموائع الحسابية. حيث تم استخدام طريقة الحجوم المحدودة فى حل معادلات نافير استوك فى وجود القوى الكهرومغناطيسية (قوى لورنتز). بالإضافة إلى معادلة الطاقة مع الأخذ فى الاعتبار تأثير الطاقة المتبددة نتيجة لتأثير جول وتأثير اللزوجة.

تم تطبيق معادلة التدويم ودالة السريان لتجزئة معادلات الموديل. وتم حل المعادلات باستخدام طريقة الحذف لجاوس، وتم الحصول على القوى الكهرومغناطيسية المؤثرة على السريان باستخدام معادلة ماكسويل ومعادلة أوم. تم استخدام برنامج فورتران يعمل على حل المعادلات الجبرية غير الخطية للموديل ، حيث تم الحصول على توزيع لسرعة السريان ثنائى الاتجاه لأرقام هارتمان مختلفة مع ثبوت رقمى رينولدز ودارسى.

تم حساب توزيعات السرعة وخطوط درجات الحرارة ، كما تم رسم منحنيات تغير رقم ناسلت مع تغير رقم هارتمان فى حالة وجود أو عدم وجود مادة مسامية. تم اختبار الموديل لمدى كبير من أرقام هارتمان ودارسى فى حدود رقم رينولدز من (10: 2000)، والموديل صالح لمدى كبير من قيم المعاملات المؤثرة كرقم براندتل وكيرشوف ورقم إيكرت. تم دراسة تأثير رقم دراسى بين القيم ( $10^{-1}$ :  $10^{-8}$ ) والنسبة بين معاملات التوصيل الحرارى لكل من المادة المسامية والمائع المستخدم (1: 300). تم مقارنة النتائج التى تم الحصول عليها مع نتائج عمليه ونظرية لأبحاث أخرى منشورة لإختبار صلاحية الموديل وقد أظهرت المقارنة توافق جيد.

### Abstract

This study aims to investigate the effects of electromagnetic fields on two-dimensional incompressible flow and heat transfer of an electrically conducting fluid flowing in a rectangular channel saturated with a porous medium. A numerical solution of the governing partial differential equations is obtained using finite volume method.

The Vorticity stream function formulation is applied to eliminate pressure as a variable in the model equations. The algebraic equations are solved by using the Gauss-elimination method. The model equations are solved using a self-written FORTRAN CODE, which solve the nonlinear algebraic equations.

The velocity and temperature contours were computed and illustrated. The graphs for Nusselt number are presented for different Hartmann numbers. The model is valid for a laminar flow ( $Re= 10 - 2000$ ) with a wide range of the affected parameters  $Ha$ ,  $Gr$  and  $Ef$  taking into account the effect of Joule and viscous dissipating energy. The calculations are valid for any values for  $Pr$ ,  $Gr$  and  $Ec$ .

To examine the validity of the proposed model, the obtained numerical results have been compared with available published experimental, analytical, and theoretical ones. The comparison shows good agreement between them.

### Keywords

Mhd; porous medium; conducting fluid; finite volume

Nomenclatures	
B, B <sub>o</sub>	Applied magnetic field Intensity, <i>Tesla</i>
C	Forschheimer; inertia coefficient
c <sub>p</sub>	Specific heat, <i>Kj/kg.°k</i>
D <sub>a</sub>	Darcy number
D <sub>h</sub>	Hydraulic diameter, m
E	Electric strength field, <i>volt/m</i>
Ec	Eckert Number
Ef	External electric field vector
g	Gravitational acceleration, <i>m/sec<sup>2</sup></i>
Gr	Grashof number
h	Convection heat transfer coefficient, $\frac{watt}{m^2 \cdot k}$
H	Channel height, <i>meter</i>
H <sub>a</sub>	Hartmann number
J	Electric current density, <i>A/m<sup>2</sup></i>
k <sub>f</sub>	Thermal conductivity, <i>W/°k</i>
l, L	Dimensional, dimensionless length, <i>m, (-)</i>
L <sub>f</sub>	Lorentz force, <i>Newton</i>
Nu	Local Nusselt number
P	Pressure, <i>Pascal</i>
P <sub>r</sub>	Prandtl number
Q	Heat input, <i>Joule</i>
q''	Heat source power per unit volume <i>W/m<sup>3</sup></i>
Re	Reynolds's number
T	Temperature, <i>°k</i>
u, v	Dimensional horizontal and Vertical velocities, <i>meter/sec</i>
U, V	Dimensionless horizontal and vertical velocities
x, y, z	Dimensional coordinates, <i>m</i>
X, Y, Z	Dimensionless coordinates

Greek symbols	
$\nu$	Kinematic viscosity <i>m<sup>2</sup>/s</i>
$\theta$	Dimensionless temperature
$\rho$	Density, <i>kg/m<sup>3</sup></i>
$\psi$	Dimensionless stream function
$\omega$	Dimensionless Vorticity
$\sigma$	Electrical conductivity, <i>1/Ohm. m</i>
$\alpha$	Thermal diffusivity of the fluid <i>m<sup>2</sup>/s</i>
$\phi$	porosity of the porous media
$\Phi$	General variable
$\beta$	Coefficient of volumetric thermal expansion of the fluid, <i>1/°k</i>

Subscripts	
<i>avg</i>	Average
Eff	Effective
F	Fluid
loc	Local
m	Mean
s	Porous material
tot	Total
w	Wall

Abbreviations	
EHD	Electrohydrodynamics
EMFD	Electromagnetofluid dynamics
FVM	Finite volume method
MHD	Magnetohydrodynamics
PIV	Particle image velocimetry

## 1. Introduction

The study of fluid flow containing electric charges under the influence of an externally applied electric field and negligible magnetic field is known as Electrohydrodynamics or EHD. The study of fluid flow influenced only by an external magnetic field is known as Magnetohydrodynamics or MHD. While the study of fluid flow under the combined influence of the externally applied electric and magnetic fields often called Electromagnetohydrodynamics **EMHD** or Electromagnetofluid dynamics. EMFD.

Formally, EMHD deal with the combined effects of electrically conducting fluids and electromagnetic forces. This is area of research is considered since the late 1930s.

EMHD addresses all phenomena related to the interaction of electric and magnetic fields with electrically conducting fluids. When an electrically conducting fluid moves through a magnetic field, it produces an electric field and subsequently an electric current. The interaction between the electric current and electromagnetic fields creates a body force, called the Lorentz force, which acts on the fluid itself. In this case, the phenomenon is known as magnetohydrodynamics MHD, but if the Lorentz force is created due to an external electric and magnetic field, it is known as Electromagnetohydrodynamics EMHD. Brian H. Dennis and George Dulikravich, [1], illustrated that effects of Joule heating and reverse pressure gradient were correctly predicted with their algorithm that been applicable to arbitrary planar flow configurations. The Lorentz force tends to suppress turbulence to a certain extent and modify the flow field.

EMHD flow control provides a prospective method that could be used in many industrial applications, ranging from power generation, propulsion system to hypersonic vehicles and atmospheric reentry vehicles, Setsuo Takezawa et al. [2].

There are two major areas of development concerning MHD: infusion technology, namely stable plasma confinement in the reactor, and the removal of heat from blankets using liquid metal coolants such as lithium-lead eutectic. For that reason, in a fusion reactor, a magnetic field has much higher importance than in other engineering applications. The designer must therefore know the effects of strong magnetic fields on the efficiency of heat transfer, pressure drop (in a variety of geometries such as duct and expansions), velocity profiles and flow turbulence.

Servati et al. [3] investigated the effects of uniform vertical magnetic field on the flow pattern and fluid–solid coupling heat transfer in a channel, which partially filled with a porous medium by utilization of the Lattice Boltzmann Method (LBM).  $\text{Al}_2\text{O}_3$ –water Nanofluid as a working fluid with temperature sensitive properties was forced to flow into the channel. In accordance with the results, by raising the nanoparticle volume fraction, average temperature and velocity at the outlet of the channel increase and the average Nusselt number rises dramatically. In addition, the increase of the Hartmann number led to the slow growth in the average Nusselt number, although the outlet average temperature and velocity shows a little drop.

Nakaharai et al. [4] carried out experimental studies on the impact of a transverse magnetic field on the local and average heat transfer of an electrically conducting, turbulent fluid flow with a high Prandtl number. The mechanism of heat transfer modification due to magnetic field was considered with the aid of available numerical simulation data for the turbulent flow field. The influence of the transverse magnetic field on the heat transfer was to suppress the temperature fluctuation and to steepen the mean temperature gradient in near-wall region in the direction parallel to the magnetic field. The mean temperature gradient was not influenced compared to the temperature fluctuation in the direction vertical to the magnetic field.

Yokomine et al. [5] conducted an investigation of MHD effects on Flibe stimulant fluid (aqueous potassium hydroxide solution) flows. They concluded that treatment of temperature field, as a passive scalar in traditional numerical simulation becomes an unreasonable assumption under magnetic field.

In recent years, application and technological development of Nanomaterials have been growing rapidly worldwide in engineering industries and

academic fields. The physical properties of Nanomaterials are reflected in the areas of heat transfer, electricity, magnetism, and mechanics. However, major problems associated with suspensions, such as sedimentation, clogging, fouling, erosion, and high-pressure drop prevented the usual nanoparticle slurries to be used as heat transfer fluids and made them unsuitable for some applications.

Chang et al. [6] carried out experimental investigations of the effect of an additional magnetic field on the stability of CuO-water Nanofluid. Under the influence of a strong magnetic field, the longer the performance time, and the more apparent, the sedimentation phenomenon will be owing to the aggregation of the nanoparticles. However, the performance frequency has a relatively slight effect on the CuO-water Nanofluid.

In last years, growing interest has been bayed to study MHD effects with and without the presence of porous media on forced and natural convection. Such interest in the topic was due to the large number of possible technological applications, like in metallurgy, where the quality of the materials, produced in the regime of controlled crystal growth, can be influenced by the effect of external electromagnetic fields. Recently been increased the efforts towards the realization of nuclear fusion machines. The effects of an EMHD in liquid metal flows were studied to design properly critical components, e.g. blankets of reactors, such studies could be found in Sidorenkov et al. [7], Kummamaru et al. [8], Mao et al. [9], Sharma and Singh [10] and Vetcha et al. [11].

For the natural convection problem solution, Aslan [12] developed and investigated a 2D nonlinear incompressible magnetohydrodynamics code to solve the steady 2D natural convection problems. The developed code can be accurately used for the solutions of MHD equations.

The heat transfer by mixed convection with the effect of

electromagnetic fields was investigated in many studies, e.g. Saleh and Hashim [13], Umavathi et al. [14], where the fully developed mixed MHD convection in vertical channels was investigated. They studied and presented graphically the effect of various parameters such as Hartmann's number, aspect ratio and buoyancy parameter with considering the effect of viscous dissipation and Joule heating.

The steady laminar flow of electrically conducting incompressible fluid between two parallel plates of a channel in the presence of the magnetic field was investigated by Ganesh and Krishnambal [15] and the solution for the case of low Reynolds number and Hartmann's number was discussed. Expressions for velocity components and the pressure were obtained.

In horizontal channels, Moh. Amro [16], investigated numerically and experimentally the EMHD flow without porous media using PIV laser system; the velocity profile and its distribution measured in many cases. In addition to; the temperature distribution, local and average Nusselt number was obtained numerically using finite volume method and EMHD FORTRAN code. Linga and Murty [17] investigated the effect of magnetohydrodynamics in mixed convection. They investigated the MHD heat transfer in fully developed viscous conductive flow of an ionized gas taking into account different geometrical considerations.

The present work is a 2D numerical investigation of EMHD mixed convection heat transfer in a horizontal channel saturated by porous media. The objective of the present work is to quantify the effects of the electromagnetic fields in the flow and heat transfer with the presence of porous media. Also, the effect of operating dimensionless parameters as  $Re$ ,  $Ha$ , on the fluid flow and heat transfer characteristics are considered.

## 2. Mathematical Modeling

The Electromagnetohydrodynamics EMHD mixed convection flow through the two-dimensional channel is assumed to be represented by a steady, viscous, incompressible, and laminar. The effect of thermal radiation is neglected. The considered governing equations are the continuity, momentum and energy equations. Constant thermo-physical properties have been assumed.

As shown in this Fig. (1), the electrically conducting fluid flows in the X direction, through a rectangular channel of 100 mm width, and 20 mm height. A constant transverse magnetic field is imposed in the Y-direction and a constant DC external electric field is applied orthogonally to the direction of flow and magnetic field.

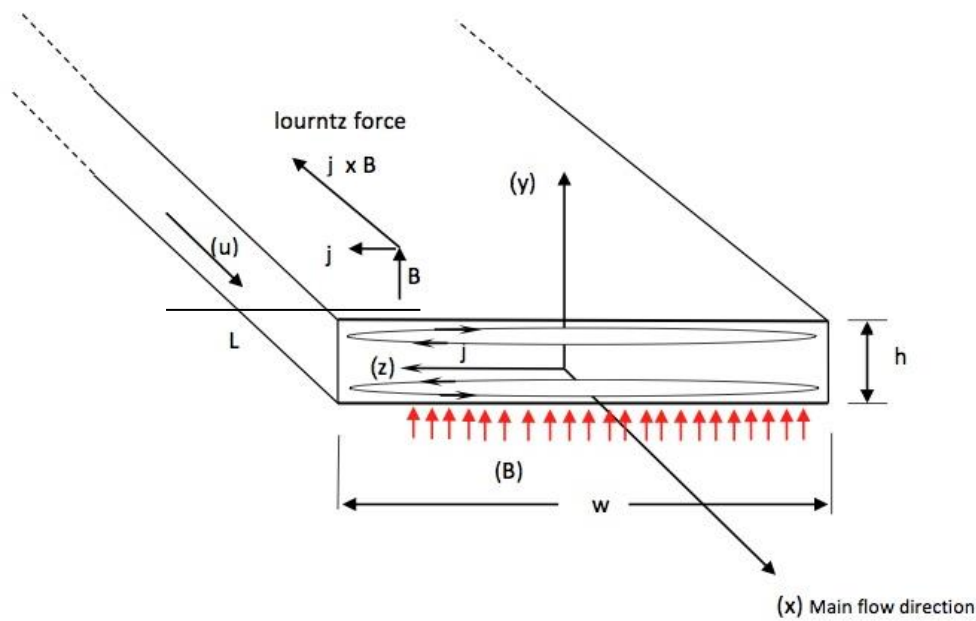


Fig.1. Physical configuration and coordinates system

### 2.1-EMHD Fluid Flow through Porous Channel:

It is assumed that the flow is steady, two-dimensional, Newtonian, incompressible and laminar flow. The porous medium is considered to be homogeneous and isotropic and in local thermodynamic equilibrium. The effect of thermal radiation on the heat transfer is negligible. The conservation equations for the flow through porous media are based on a general flow model, which includes the effects of flow inertia as well as the friction caused by macroscopic shear studied by Vafai, and Tien [18]. This generalized flow model is also known as

Brinkman-Forschheimer-extended Darcy model [19]. The governing equations for fluid flow through the porous media are:

Continuity equation:

$$\frac{\partial u}{\partial x} + \frac{\partial v}{\partial y} = 0 \quad (1)$$

Momentum equations:

X-Direction:

$$\frac{1}{\phi^2} \left[ u \frac{\partial u}{\partial x} + v \frac{\partial u}{\partial y} \right] = -\frac{1}{\rho} \left( \frac{\partial p}{\partial x} \right) - \left[ \left( \frac{C}{\sqrt{k}} \right) |v| + \frac{v}{k} \right] u + v \left( \frac{\partial^2 u}{\partial x^2} + \frac{\partial^2 u}{\partial y^2} \right) + (J \times B)_x \quad (2)$$

Y-Direction

$$\frac{1}{\phi^2} \left[ u \frac{\partial v}{\partial x} + v \frac{\partial v}{\partial y} \right] = -\frac{1}{\rho} \left( \frac{\partial p}{\partial y} \right) - \left[ \left( \frac{C}{\sqrt{k}} \right) |v| + \frac{v}{k} \right] v + v \left( \frac{\partial^2 v}{\partial x^2} + \frac{\partial^2 v}{\partial y^2} \right) + g\beta(T - T_0) \quad (3)$$

Taking into considerations that, in a boundary layer, the velocity component in the direction along the surface,  $u$ , is much larger than that normal to the surface,  $v$ , and gradients normal to the surface are much larger than those along the surface, the viscous term of the velocity could be neglected, and then the energy equations are:

$$u \frac{\partial T}{\partial x} + v \frac{\partial T}{\partial y} = \alpha_{\text{eff}} \left[ \frac{\partial^2 T}{\partial x^2} + \frac{\partial^2 T}{\partial y^2} \right] + \frac{v}{c_p} \left[ \frac{\partial u}{\partial y} \right]^2 + \frac{|J|^2}{\sigma} \quad (4)$$

Where;

$u$  and  $v$  are the average (seepage, filtration) velocity components in the  $x$  and  $y$  directions

$|v|$  is the resultant velocity, absolute value,  $|v| = \sqrt{u^2 + v^2}$

$\phi$  is the porosity of the porous media,  
 $\phi = \frac{\text{void volume}}{\text{total volume}} = \frac{V_f}{V_T}$

$V_f$  is the volume of the fluid.

$V_T$  is the total volume of the medium  
 $K$  is the permeability.

$C$  is the Forchheimer inertia coefficient,  
 $C = \frac{1.75}{\sqrt{150}\phi^{1.5}}$

The effective thermal diffusivity of the fluid saturated porous media,  $\alpha_{\text{eff}}$ , is defined as  $\alpha_{\text{eff}} = k_{\text{eff}}/(\rho c)_f$ , where  $k_{\text{eff}}$ , refers to the effective thermal conductivity of the fluid saturated porous media which is calculated according to the definition:

$$k_{\text{eff}} = \phi k_f + (1 - \phi) k_s$$

Where:

$k_f$  Is the thermal conductivity of the fluid.

$k_s$  Is the thermal conductivity of the porous material.

It has been found that setting the effective viscosity of the fluid-saturated porous media equal to the viscosity of the fluid  $\nu$ , provided good agreement with experimental data, Lundgren [20]. This approximation is adopted in the present work. In addition, the effect of thermal dispersion in the porous matrix is assumed to be constant and incorporated in the effective thermal conductivity for the simplicity in presentation of the results.

Where:

$J \times B$  is the electromagnetic Lorentz body force.

$\frac{|J|^2}{\sigma}$  is the dissipating energy due to Joule heating from electric field.

The second term in the right hand side of the energy equation represent the energy dissipating due to the viscous losses and could be neglecting for the Newtonian fluid. As a means of validating electric field and Lorentz, force calculations, the steady and two-dimensional flow of an electrically conducting, viscous, incompressible fluid within a rectangular duct with both parallel perfectly conducting and insulating walls, has been considered. A constant transverse magnetic field was applied. The combination of parallel pairs of electrically conducting and insulating walls allows a current that will accelerate the flow close to the non-conducting walls whilst retarding it elsewhere. In this case, the standard Navier-Stokes equations were solved, with the addition of a bulk damping resistance due to the porous structure that was represented according to Brinkman-Forschheimer-extended, Darcy model [19], and a Lorentz force, and heat dissipating according to the followings;

$$J \times B = \sigma(E + u \times B) \times B = \sigma B^2 \left( \frac{E}{B} - u \right), \quad \frac{J^2}{\sigma} \\ = \sigma B^2 \left( \frac{E}{B} + u \right)^2 \quad (5)$$

## 2.2-The Dimensionless Form of the Governing Equations

The governing equations of continuity, momentum and energy equations can be transformed to the dimensionless form, with the dimensionless variables defined as:

$$X = \frac{x}{H}, \quad Y = \frac{y}{H}, \quad U = \frac{u}{U_0}, \\ V = \frac{v}{U_0}, \quad P = \frac{p}{\rho U_0^2}, \quad \theta = \frac{T - T_0}{T_w - T_0}, \quad E_f = \frac{E}{B \cdot U_0}$$

Then, the governing equations can be written as:

Continuity equation:

$$\frac{\partial U}{\partial X} + \frac{\partial V}{\partial Y} = 0 \quad (6)$$

Momentum equations:

X-direction:

$$\frac{1}{\phi^2} \left[ U \frac{\partial U}{\partial X} + V \frac{\partial U}{\partial Y} \right] = -\frac{\partial P}{\partial X} + \frac{1}{Re} \left[ \frac{\partial^2 U}{\partial X^2} + \frac{\partial^2 U}{\partial Y^2} \right] - \xi \left[ \left( \frac{C}{\sqrt{D_a}} \right) |V| + \frac{1}{Re D_a} \right] U + \frac{H_a^2}{Re} (E_f - U) \quad (7)$$

Y-direction:

$$\frac{1}{\phi^2} \left[ U \frac{\partial V}{\partial X} + V \frac{\partial V}{\partial Y} \right] = -\frac{\partial P}{\partial Y} + \frac{1}{Re} \left[ \frac{\partial^2 V}{\partial X^2} + \frac{\partial^2 V}{\partial Y^2} \right] + \frac{Gr}{Re^2} \theta - \xi \left[ \left( \frac{C}{\sqrt{D_a}} \right) |V| + \frac{1}{Re D_a} \right] V \quad (8)$$

Energy equations:

$$U \frac{\partial \theta}{\partial X} + V \frac{\partial \theta}{\partial Y} = \frac{R_k}{Re Pr} \left[ \frac{\partial^2 \theta}{\partial X^2} + \frac{\partial^2 \theta}{\partial Y^2} \right] + \frac{Ec}{Re} \left[ \frac{\partial U}{\partial Y} \right]^2 + \frac{Ec H_a^2}{Re} (E_f + U)^2 \quad (9)$$

Where

$D_h = \frac{4 \cdot (\text{area})}{\text{witted perimeter}}$  is the hydraulic diameter,  $Re = \frac{U D_h}{\nu}$  is Reynolds's number,  $Gr = g \beta L^3 \Delta T / \nu^2$  is Grashof number,  $Pr = \nu / \alpha$  Prandtl number,  $Ec = u^2 / c_p \Delta T$ , is Eckert number,  $Ha^2 = \frac{\sigma B^2 D_h^2}{\mu}$  is Hartmann's number and  $D_a = \kappa / h^2$  is Darcy number.

The difficulty associated with the determination of the pressure has led to methods that eliminate the pressure from the two momentum equations by cross differentiation, which lead to the Vorticity-transport equation. This, when combined with the definition of a stream function for steady two-dimensional fluid flow, is the basis of the well-known "stream function/ Vorticity method". The stream function and vorticity are defined in the usual way as:

$$U = \frac{\partial \psi}{\partial Y}, \quad V = -\frac{\partial \psi}{\partial X}, \quad \omega = \frac{\partial V}{\partial X} - \frac{\partial U}{\partial Y} \quad (10)$$

Where  $\psi$  and  $\omega$  are dimensionless stream and vorticity functions.

Substituting the value of both the dimensions velocity components U and V from the equation (7) and in equation (8) an equation for the vorticity-stream function is obtained as:

$$-\omega = \frac{\partial^2 \psi}{\partial X^2} - \frac{\partial^2 \psi}{\partial Y^2} \quad (11)$$

The pressure is eliminated between Eq.7 and Eq. 8 by differentiating (7) with

respect to Y and equation (8) with respected to X and subtracting the results...

The resulting equation is called the momentum equation of vorticity and has the form:

$$\frac{1}{\phi^2} \left[ U \frac{\partial \omega}{\partial X} + V \frac{\partial \omega}{\partial Y} \right] = \frac{1}{Re} \left[ \frac{\partial^2 \omega}{\partial X^2} + \frac{\partial^2 \omega}{\partial Y^2} \right] + \frac{H_a^2}{Re} \left[ \frac{\partial U}{\partial Y} \right] + \frac{Gr}{Re^2} \frac{\partial \theta}{\partial X} - \left[ \left( \frac{C}{\sqrt{D_a}} \right) |V| + \frac{1}{Re D_a} \right] \omega - \frac{C}{\sqrt{D_a}} \left[ V \frac{\partial |V|}{\partial X} - U \frac{\partial |V|}{\partial Y} \right] \quad (12)$$

Eqs 6-12 represent the model governing equations, which are functions of the dimensions the vorticity  $\omega$ , temperature  $\theta$ , the stream function  $\psi$ , and velocities U and V.

The local Nusselt number along the surface may be expressed with the local convective heat transfer coefficient as:

$$Nu_{loc} = \frac{h D_h}{K_{eff}} = -Re_k \frac{\partial \theta}{\partial Y} \Big|_w \quad (13)$$

The average Nusselt number can be calculated as follows:

$$Nu_{avg} = \frac{1}{A} \int Nu_{loc} \cdot dA \quad (14)$$

Where, A is the surface area exposed to the fluid. The boundary conditions for the present problem are specified as follows:

At the inlet:

At all solid boundaries other than top

$$U = 1, \quad V = 0, \quad \theta = 0 \quad \text{for } X = 0 \text{ and } 0 \leq Y \leq 1$$

and bottom wall:  $U = 0; V = 0; \partial \theta / \partial N = 0$

At the top and bottom wall:  $U = V = 0, \theta = 1$

At the channel exit section U, V and  $\theta$  are extrapolated.

Where N is the non-dimensional distances either X or Y direction, acting normal to the surface.

### 3- Numerical solution:

A finite volume method FVM, procedure discussed by Patankar [21] and Versteeg and Malalasekera [22] has been used for discretizing the governing equations. The computational domain in two dimensions has been discretised using control volumes of uniform size. Convection-diffusion terms have been treated by the central differencing scheme.



The governing equations are integrated over the control volume with the use of linear interpolation inside the finite element, and the obtained algebraic equations are solved by the Gauss- Seidel method. The above-mentioned numerical method has been implemented in a self-written FORTRAN computer code which, solve non-linear partial differential equations in two dimensions. The domain is subdivided into a number of control volumes, each associated with a grid point. The governing equations are integrated over control volume, the following general form for the diffusion –convection equation, (13) is used to solve the model equations:

$$\frac{\partial}{\partial X}(\Phi U) + \frac{\partial}{\partial Y}(\Phi V) = \frac{\partial}{\partial X}\left(\Gamma \frac{\partial \Phi}{\partial X}\right) + \frac{\partial}{\partial Y}\left(\Gamma \frac{\partial \Phi}{\partial Y}\right) + (S_u + S_p \Phi) \quad (15)$$

The two terms in the left-hand side of equation (13), are the convection terms, while the first term and second terms of the right-hand side represent the diffusion terms, the third is the source term. The obtained algebraic equations of the Vorticity, stream function, temperature, and velocity components are solved using the Gauss-eliminating method. An iterative solution procedure is employed to obtain the steady state solution of the considered problem. The convergence criteria used for all field variables ( $\Phi = \psi, \omega, \theta$ ) for every point is:

$$\varepsilon = \frac{\sum_{j=1}^M \sum_{i=1}^N |\Phi^{n+1} - \Phi^n|}{\sum_{j=1}^M \sum_{i=1}^N |\Phi^{n+1}|} < 10^{-5} \quad (15)$$

where  $\varepsilon$  is the tolerance; M and N are the number of grid points in the x and y directions, respectively.

In order to ensure the grid-independence solutions, a series of trial calculation was conducted for different grid size: 51x101, 101x201, 151x251 and 401x501. The results of the average Nusselt numbers using different grid arrangements are 5.06, 5.1575, 5.2565 and 5.2573. It observed that difference between the result of the grid 151x251 and that of the grid 401x501 is less than 0.015%.

Consequently, to optimize appropriate grid refinement with computational efficiency, the grid 151x251 is chosen for all computation.

### 4. Model Validation:

The accuracy of FVM and FORTRAN code was tested against the analytical solution for Poiseuille-Hartmann flow of a conducting and viscous fluid between two stationary plates with uniform external magnetic field orthogonally to the plates. Assuming the wall direction under the influence of a constant pressure gradient, Fig. 2 illustrated the computed and analytical velocity profile. It appears in a very good agreement.

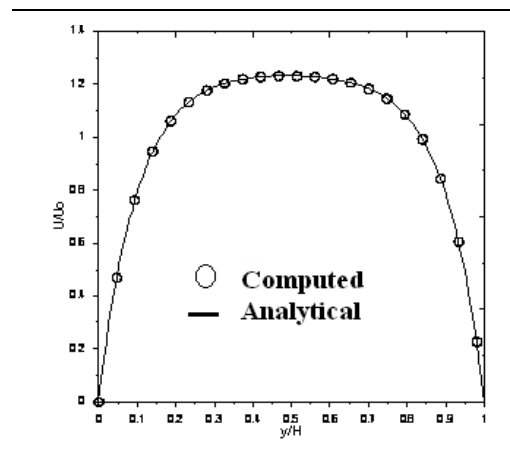


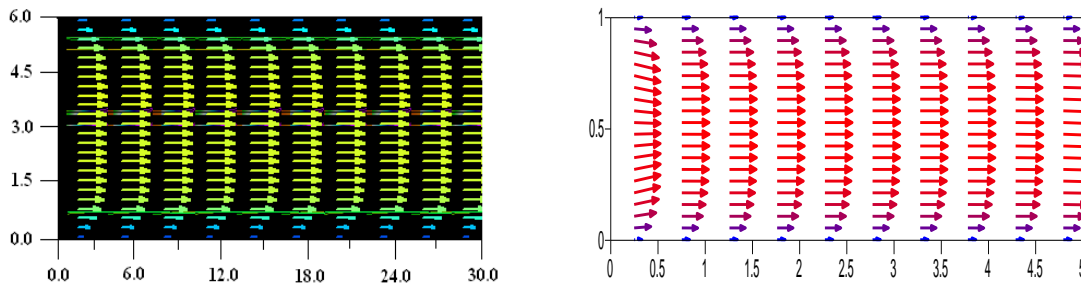
Fig. 2. Analytical and computed velocity profile

at  $y=0$  and  $y=H$  and that the fluid velocity on the walls is zero and that the fluid moves in X

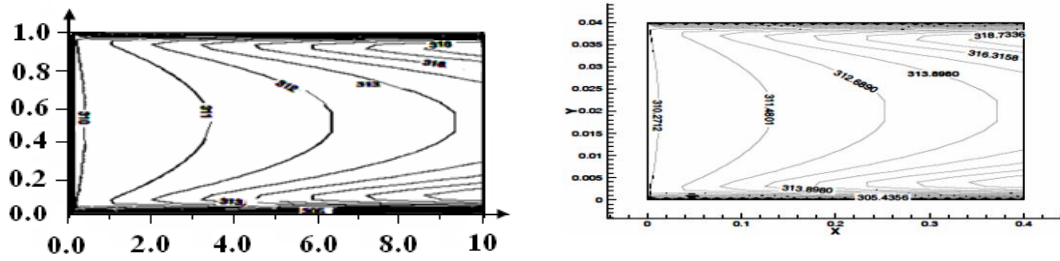
The model was validated tests against the experimental results obtained by PIV laser system by Moh. Amro [16] for the fully developed flow. One note that the velocity has the maximum value in the most of the channel regions and the boundary layer is compressed due to the action of the Lorentz body force, which creates a new boundary layer proportional to the inverse of the Hartmann's number. as shown in Fig.3 (a-b). The accuracy of the numerical model is also verified by comparing the temperature contours of the present work and the temperature contours Dulikravich.

This could be found in Fig. 4 (a-b). The comparison shown a good agreement

calculated by Brian H.Dennis.and.George,.[1].



*a. V-profile experimental (PIV), (L/H=5)*      *b. V- profile computed with code*  
**Fig.3. Comparison between (PIV) measured distribution by El-Zahaby et al and computed velocity profiles.**



*a. Computed temperature, contour, present work*      *b. Temperatures contour Dulikravich [18]*  
**Fig.4. Comparison between temperature contours for the present work (a) and Dulikravich [18] (b), at (Gr/Re = 10, Ha = 1000).**

### 5. Results and discussion:

In Fig. 5 the velocity fields were presented at constant Reynolds's number,  $Re = 50$  for different values of the Hartmann number from, zero – 3000. It appears that the maximum velocity value decreases as the Hartmann number increases. In addition, thickness decreases when Hartmann number increases and the profile are flat. These features are due to the higher values for the Lorentz force and buoyancy force that create the high values of velocity gradient near the walls. These features increase as Hartmann number increases. In Fig. 5, the velocity profiles shown in a different Hartmann number. It shows that the maximum velocity decreases and the profile become more flatting as the Hartmann number increases.

As the Hartmann increases the boundary layer thickness decreases. This decreases also the thermal boundary layer thickness and this enhancement the heat transfer rates.

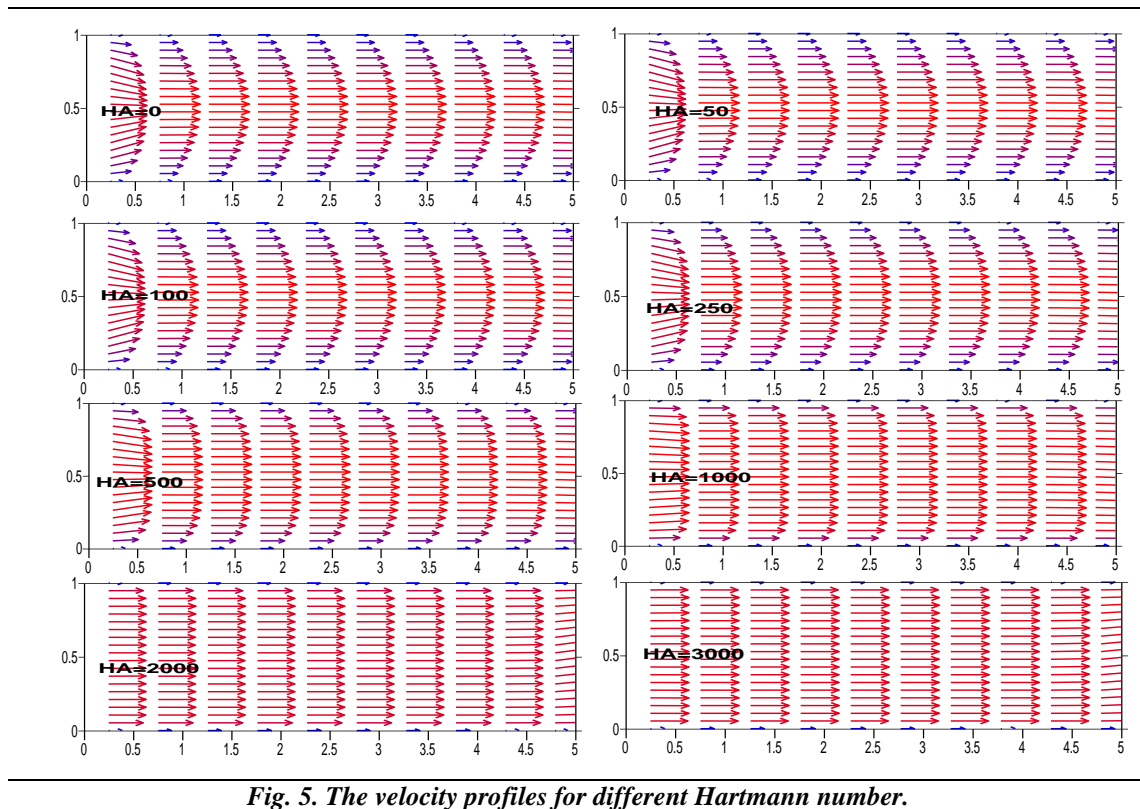


**Fig. 5. The velocity profiles for different Hartmann number.**

Fig. 6 represents the temperature contours at a constant Reynolds number ( $Re = 50$ ) for different values for the Hartmann number ( $Ha = \text{zero} - 3000$ ). All temperature contours in this case computed with no effect to the external electric field parameter ( $Ef = 0$ ). Results showed that as the Hartmann number increases, the Lorentz force created by the coupling between the induced electric field and the applied magnetic field increases. This force action opposite the flow direction and alters the heat transfer characteristics, due to the decelerating of the flow velocity. A direct result of the increasing of the induced current is creating an internal heat flux in the flow, so the temperature distribution and temperature difference between the inlet temperature  $T_0$  and the fluid temperature  $T$  at any position is larger than the difference between the inlet and wall temperature. Due to that, as the Hartmann's number,  $Ha$  increases the average Nusselt number, does not decrease.

Fig.7 illustrated temperature distribution at a constant Reynolds number

( $Re=50$ ) and different values for the Hartmann number ( $Ha = \text{zero}-3000$ ) and external electric field parameter ( $Ef=\text{zero}$ ), with a porous medium of Darcy number  $Da = 10^{-5}$ . The internal heat flux increases also with increasing the Lorentz force due to Hartmann number,  $Ha$  increase. It is obvious that the effect of Hartmann number  $Ha$ , on internal heat flux increases in case of porous medium of Darcy number  $Da = 10^{-5}$  than Un-porous, so the rate if heat transfer also increases, and as a consequence, the Nusselt number.increases.

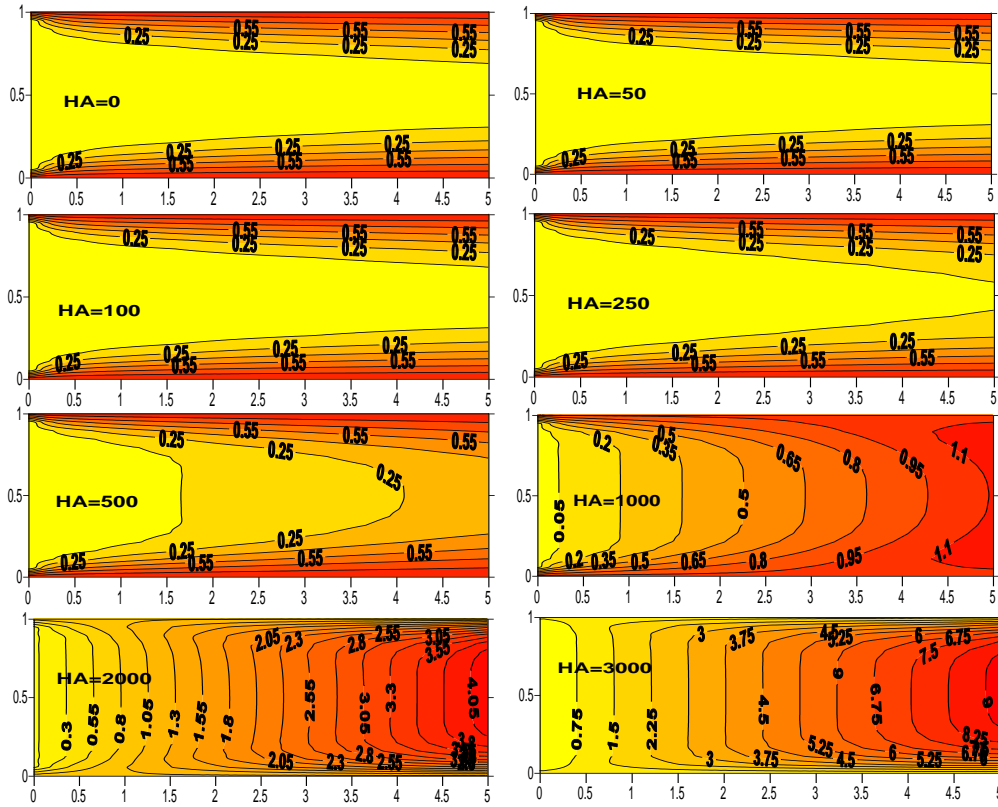


Fig.6. Temperature contours due to  $Ha$  variation for  $(Re = 50, Ef = 0)$ .

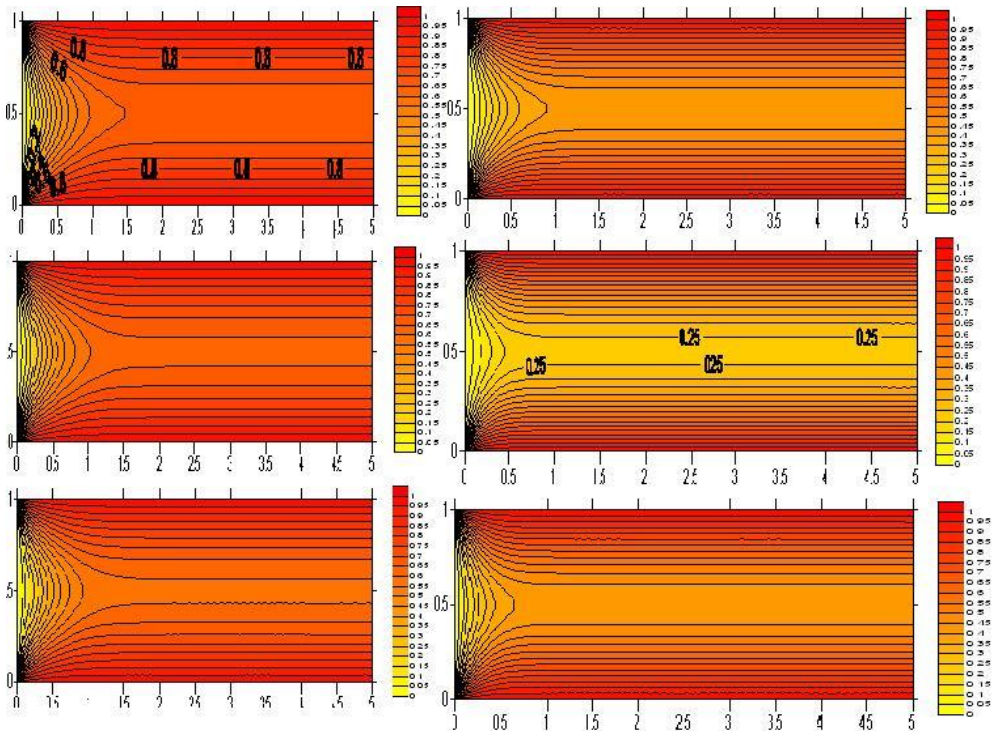


Fig. 7. Temperature distribution at a constant Reynolds number  $(Re=50)$  and different values for the Hartmann number  $(Ha = zero-3000)$  and external electric field parameter  $(Ef=zero)$  and Darcy number  $Da = 10^{-5}$

### Variation of Nusselt number with Hartmann number

As shown in Fig. 8 the average Nusselt number, variation is represented by the Hartmann number of different cases for the external electric field parameter at the constant Reynolds number,  $Re = 50$ . Generally the average Nusselt number,  $Nu_{avg}$  decreases with increases in Hartmann if the flow under the induction electric (magnetic) field only. The average Nusselt number decreases sharply if the electric field parameter has higher values, as  $Ef = 4$ . This is due to the higher values for the Joule dissipating energy. Because of this, the heat transfer alters. When the value of external electric field parameter  $Ef$  is held at constant value more than zero but less than unity, it is enhanced the heat transfer and the Nusselt number is increased.

In the case of constant wall temperature, the application of

electromagnetic fields when  $Ef = 0.5$  increases the heat transfer approximately by 1.667 times its value. When the external electric field parameter  $Ef$ , equals unity the Joule heating dissipating energy is totally deleted. Just the external electric field parameter increases over than unity, the Joule dissipating energy returns to increase again, as the case represents with  $Ef = 4$ .

The relation between the Nusselt number  $Nu$  and the Hartmann number  $Ha$  depends on the value of the external electric field parameter, when the effect of external electric field is taken into consideration.

Fig. 9 represents the variation of local Nusselt number with the channel length,  $X$ . One find that, as channel length increases, the local Nusselt number decreases. Moreover, increasing in Hartmann number,  $Ha$  decreases the local Nusselt number for the same channel length.  $X$ .

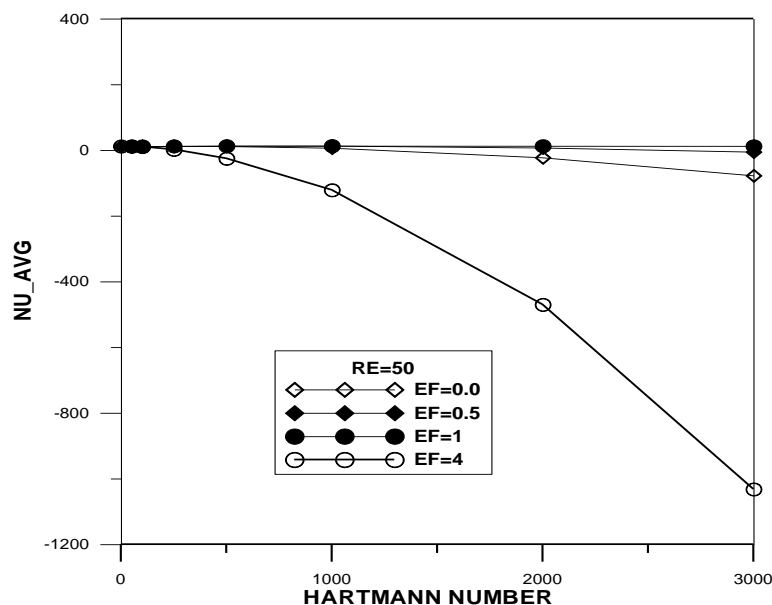


*Fig. 8. Relation between average Nusselt number,  $Nu_{avg}$  and Hartmann number for constant Reynolds number  $Re=50$  and different values for the external electric field parameter*

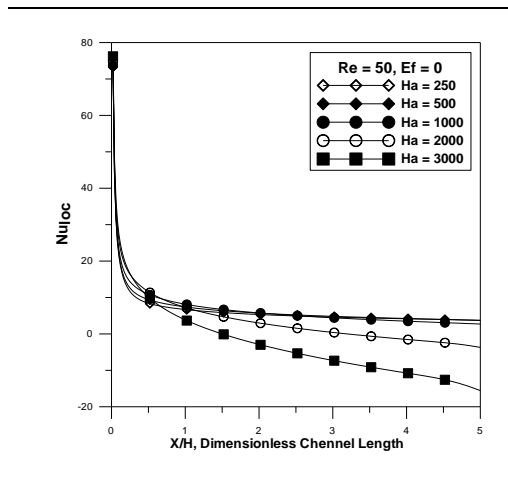


**Fig. 9. Relation between  $Nu_{loc}$  and Dimensionless Channel Length,  $x/H$ .**

Furthermore, the same variation trend of local Nusselt number with the channel length,  $X$  was observed as shown in Fig. 10 when the relation between  $Nu_{loc}$  and Dimensionless Channel Length,  $x/H$ , was drawn for a constant Reynolds number ( $Re=50$ ) and different values for the Hartmann number ( $Ha = \text{zero}-3000$ ) and external electric field parameter ( $Ef=\text{zero}$ ) with Darcy number  $Da = 10^{-5}$ . As channel length increases, the local Nusselt number decreases. The Hartmann number,  $Ha$  effect on local Nusselt number variation was less with porous medium for a Darcy number  $Da = 10^{-5}$ .

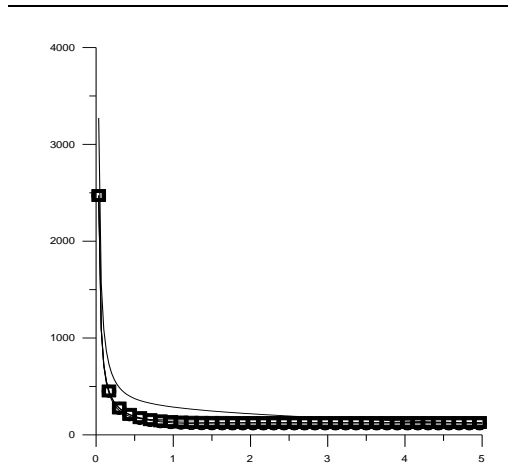


**Fig. 10. Local Nusselt numbers along the length of the channel for different values for  $Re=50$ , Hartmann number ( $Ha = \text{zero} - 3000$ ), and  $Da = 10^{-5}$**

## 6. Conclusions

The Electromagnetohydrodynamics mixed convection flow through a rectangular channel solved numerically. The governing equations of the model consist of the mass, momentum and energy equations. The Vorticity-stream function formulation is used and the finite volume technique was applied to discrete the model equations. The algebraic equations solved by using the Gauss-elimination method. Forced convection heat transfer to an EMHD fluid of a porous flat duct is investigated in the present work. Both Joule heating and viscous dissipation were taken into consideration. The influence of the Hartmann number, Reynolds number, Darcy number and external electric field parameter on temperature profile and local Nusselt number are discussed.

- When the value of the external electric field parameter is equal to zero, the rate of heat transfer is altering and the average Nusselt number is decreasing with the increasing of the induced electric current.
  - In case of the effect of the external electric current, the rate of heat, transfer and flow velocities depend on the current value and direction.
  - The heat transfer rate and Nusselt number are largely effective and increase with increasing of the external electric field parameter up till a certain value less than unity depends on the  $Ha$  number effect.
  - The use of porous media in the presence of electromagnetic fields increases the Nusselt number, so, the rate of heat transfer also increases
- The model is valid for any values of Prandtl, Eckert, and Grashof' numbers.

## References

[1] Brian H. Dennis and George Dulikravich "Electromagnetohydrodynamics (EMHD): Numerical Experiments in Steady Planar Flows" Copyright by ASME Journal, 2000 and AMD.

- Vol.244/MD-Vol.92, Recent Advanced in the Mechanics of Structured Continuo – 2000.
- [2] Setsuo Takezawa, Hiroshi Tamama, Kazumi Sugwawa, Hiroshi Sakai, Chiaki Matsuyama, Hiroak Morita, Hiromi Suzuki and Yoshihiro Ueyama " Operation of the Thruster for Superconducting Electromagnetohydrodynamics Propulsion Ship " YAMATO 1" Journal of the MESJ , Vol.29, No.6, March , 1995.
- [3] Ata A. Servati, koroush Javaherdeh, Hamid Reza "Magnetic field effects on force convection flow of a nanofluid in a channel partially filled with porous media using Lattice Boltzmann Method" Journal of ScienceDirect, Vol. 25, issue 2, March 2014, pages 666-675.
- [4] H. Nakaharai, J. Takeuchi, T. Yokomine, "The influence of a magnetic field on turbulent heat transfer of a high Prandtl number fluid" Experimental Thermal and Fluid Science 32 (2007) 23–28
- [5] T. Yokomine, J. Takeuchi, H. Nakaharai, S. Satake, "EXPERIMENTAL INVESTIGATION OF TURBULENT HEAT TRANSFER OF HIGH PRANDTL NUMBER FLUID FLOW UNDER STRONG MAGNETIC FIELD" FUSION SCIENCE AND TECHNOLOGY VOL. 52 OCT. 2007
- [6] Ho Chang1, Tsing-Tshih Tsung, Chii-Ruey Lin, "A Study of Magnetic Field Effect on Nanofluid Stability of CuO" Materials Transactions, Vol. 45, No. 4 (2004) pp. 1375 to 1378
- [7] Sergei I. Sidorenkov, Thanh Q. Hua and Hideo Araseki "Magnetohydrodynamics and Heat Transfer Benchmark Problems for Liquid-Metal Flow in Rectangular Ducts" Journal of Fusion Engineering and Design 27 (1995) 711-718.
- [8] Hiroshige Kummamaru, Satoshi Kodama, Hiroshi Hirano and Kazuhiro Itoh " Three- dimensional numerical calculations on liquid metal magnetohydrodynamic flow in Magnetic field Inlet region" Journal of Nuclear Science and technology, Vol. 41, No. 5, pp. 624-631, May 2004.
- [9] J. Mao, S. Aleksandrova, S. Molokov "Joule Heating in Magnetohydrodynamic Flows in Channels with Thin Conducting Walls" International Journal of Heat and Mass Transfer 51 (2008) 4392-4399.
- [10] P.R. Sharma and G. Singh "Numerical Solution of Transient MHD Free Convection Flow of an Incompressible Viscous Fluid along an Inclined Plate with Ohmic Dissipation "International Journal of Applied Mathematics and Mechanics 5 (5): 57-65, 2009.
- [11] N. Vetcha, S. Smolentsev and Mohamed Abdou "Theoretical Study of Mixed Convection in Poloidal Flows of DCLL Blanket" Journal of Fusion Science and Technology, vol. 56, Aug. 2009.
- [12] N. Aslan "An Incompressible Magnetohydrodynamics Solver" Journal of Theoretical and Applied Physics, 3-4, 1-9, 2010.
- [13] H. Saleh and I. Hashim, "Flow Reversal of Developed Mixed Convection in Vertical Channels" China Journal of LETT. Vol.27, No.2, 2010, 024401.
- [14] J.C. Umavathi, I.C. Liu and Prathap Kumar "Fully Developed Magneto Convection Flow in a Vertical Rectangular Duct" Journal of Heat and Mass Transfer, Vol. 47:1-11, 2011.
- [15] S. Ganesh and S. Krishnambal "Magnetohydrodynamic Flow of Viscous Fluid between Two Parallel Porous Plates" Journal of Applied Sciences 6 (11): 2420-2425, 2006.



- [16] Moh. Amro, "Electric Field Effect on Fluid Flow And Heat Transfer in Channels" PhD Thesis, 2013
- [17] T. Linga Raju and P.S. R. Murty " MHD Heat Transfer Aspects Between Two Parallel conducting Porous Walls in a Rotating System, with Hall Currents" African Journal of Mathematics and Computer Science Research Vol. 4 (7), pp. 242-250 July, 2011.
- [18] K. VAFAI and C. L. TIEN "BOUNDARY AND INERTIA EFFECTS ON FLOW AND HEAT TRANSFER IN POROUS MEDIA" Int. J. Heat Mass Transfer, Vol. 24, pp. 195-203
- [19] Basant K. Jha, Muhammad L. Kaurangini "Approximate Analytical Solutions for the Nonlinear Brinkman-Forchheimer-Extended Darcy Flow Model" Applied Mathematics, 2011, 2, 1432-1436
- [20] Lundgren "Porous Media: Fluid Transport and Pore Structure", (1972).
- [21] Patanker, S. V., "Numerical Heat Transfer and Fluid Flow" Hemisphere publishing company, New York, 1980.
- [22] Versteeg, H. K. and Malalasekera, W. "An Introduction to Computational Fluid Dynamics, the Finite Volume Method", Longman Malaysia, TCP, 1995